

## WNT2 Regulates Proliferation of Mouse Granulosa Cells through Beta-Catenin1

Hong-Xing Wang<sup>2,3</sup>, Tony Y. Li<sup>2</sup>, and Gerald M. Kidder<sup>2,4,5</sup>

<sup>2</sup> Departments of Physiology and Pharmacology, Obstetrics and Gynaecology, and Paediatrics, Schulich School of Medicine and Dentistry, The University of Western Ontario, London, Ontario N6A 5C1

<sup>4</sup> Children's Health Research Institute, 800 Commissioners Road East, London, Ontario N6C 2V5

### Abstract

WNTs are secreted extracellular signaling molecules that transduce their signals by binding to G protein-coupled receptors of the frizzled (FZD) family. They control diverse developmental processes such as cell fate specification, cell proliferation, cell differentiation, and apoptosis. Although WNT signaling has been shown to be essential for development of the ovary, its mechanistic role in folliculogenesis within the adult ovary has not been studied extensively. Therefore, the objective of this study was to investigate the regulation and function of WNT2 signaling in mouse granulosa cells. Immunostaining identified WNT2 as being expressed in granulosa cells throughout folliculogenesis, but with varying signal strength: in sequential sections, WNT2 immunoreactivity was strongest in healthy antral follicles but weak in atretic follicles. Knockdown of WNT2 expression using transfected siRNA decreased the proliferation rate of granulosa cells whereas WNT2 overexpression using a recombinant viral vector enhanced their proliferation. WNT2 knockdown led to accumulation of glycogen synthase kinase-3 $\beta$  (GSK-3 $\beta$ ) in the cytoplasm but reduced the expression of  $\beta$ -catenin. Conversely, WNT2 overexpression reduced the expression of GSK-3 $\beta$  in the cytoplasm and induced  $\beta$ -catenin translocation from the membrane into the nucleus.  $\beta$ -catenin knockdown also inhibited the proliferation of granulosa cells, and neutralized the proliferation effect of WNT2 overexpression. WNT2/ $\beta$ -catenin signaling had a slight effect on the apoptosis of granulosa cells. Taken together, the data indicate that WNT2 regulates  $\beta$ -catenin localization in granulosa cells and WNT2/ $\beta$ -catenin signaling contributes to regulating their proliferation.

### Keywords

WNT; FZD; GSK-3 $\beta$ ;  $\beta$ -catenin; AXIN; proliferation; granulosa cell

---

<sup>1</sup>Funded by grant MOP-14150 from the Canadian Institutes of Health Research

<sup>5</sup>Address for correspondence: Dr. Gerald M. Kidder, Department of Physiology and Pharmacology, Dental Sciences Building, dock 15, The University of Western Ontario, London, Ontario N6A 5C1, Canada, Phone: 519-661-3132, Fax: 519-850-2562, gerald.kidder@schulich.uwo.ca.

<sup>3</sup>Present address: Department of Cancer Immunology and AIDS, Dana-Farber Cancer Institute, 44 Binney Street, Boston, MA 02115

## INTRODUCTION

WNTs are a large family of secreted, cysteine-rich glycoproteins that influence diverse functions during development, such as cell fate specification, cell proliferation, differentiation, survival and apoptosis, polarity, and migration [1, 2]. Currently, three different pathways have been found to be activated by WNT receptor activation: the canonical WNT/ $\beta$ -catenin cascade, the non-canonical planar cell polarity (PCP) pathway, and the WNT/ $\text{Ca}^{2+}$  pathway [3]. The canonical WNT pathway is well understood for its ability to regulate cell-cell adhesion and cell cycle control, and  $\beta$ -catenin is the central and essential component in this pathway [4]. The phosphorylation and stability of  $\beta$ -catenin are regulated by a cytoplasmic protein complex formed by casein kinase-1 $\alpha$  (CK1 $\alpha$ ), glycogen synthase kinase-3 (GSK3), and tumor suppressors adenomatous polyposis coli (APC) and AXIN [1, 5]. In the absence of WNT, the AXIN complex is constitutively active, promoting the phosphorylation of  $\beta$ -catenin and its proteasomal degradation [5]. In contrast, loss of function or inhibition of the AXIN complex causes activation of  $\beta$ -catenin [6]. As a result, hypophosphorylated  $\beta$ -catenin accumulates in the cytoplasm and is translocated to the nucleus where it interacts with the T-cell factor and lymphoid enhancer-binding factor (TCF/LEF) family of transcription factors to activate the transcription of target genes [7].

To date, 19 WNT members have been identified in mouse and human. WNTs have been implicated in a range of developmental processes in the mouse including the patterning of the central nervous system and limbs [3, 8]. Knockout or mutation of WNT genes causes cell proliferation defects in mice. In WNT1/WNT3a double mutant mice, the reduction in neural crest and deficiency in dorsolateral neural precursors were attributed at least in part to a cell proliferation defect [9, 10]. WNT5a has been shown to regulate the proliferation of progenitor cells in both the limb bud progress zone and the primitive streak mesoderm, while WNT7b is required for mesenchymal proliferation and vascular development in the lung [11, 12]. Similarly,  $\beta$ -catenin deficiency in mouse embryos resulted in reduced progenitor proliferation [13]. It has been demonstrated that targeted disruption of the *Wnt2* gene results in placentation defects [14]. Alteration of WNTs can also be associated with tumorigenesis. Up-regulation of WNT2 has been found in human colorectal cancer and gastric cancer, while WNT2 siRNA or monoclonal antibody could inhibit tumor growth [15–17]. WNT2 acts as an autocrine growth and differentiation factor specific for hepatic sinusoidal endothelial cells (HSECs) where it synergizes with the VEGF signaling pathway to exert its effect [18].

During the mammalian reproductive cycle, the ovary undergoes dynamic morphological changes. The different ovarian compartments are subject to both proliferation and differentiation events, and ovarian folliculogenesis requires complex regulatory mechanisms involving both endocrine and intra-ovarian signaling pathways [19, 20]. Recently, WNT signaling has been implicated in ovarian development, oogenesis, and early development. *Wnt4* deficient mice exhibit sex reversal and a paucity of oocytes in the newborn ovary, while mice null for *Fzd4* are infertile and exhibit impaired function of the corpus luteum [21, 22]. Multiple *Wnt* transcripts are localized in the different compartments of the mouse ovary: *Wnt2* and *Fzd1* are expressed in the granulosa cells while *Wnt4* and *Fzd4* are expressed in the corpus luteum [23, 24]. Our recent study of human cumulus cells revealed

the presence of the canonical WNT pathway, with WNT2 acting through its receptor FZD9 to recruit  $\beta$ -catenin into plasma membranes and promote the formation of adherens junctions [25]. It has also been reported that misregulation of WNT/ $\beta$ -catenin signaling in granulosa cells can contribute to granulosa cell tumor development [26]. However, very little is known about the function and regulation of the WNT/ $\beta$ -catenin signaling pathway in normal follicle development. This study was undertaken to explore the function of this pathway and its regulatory mechanisms in mouse granulosa cells.

## MATERIALS AND METHODS

### Ovary Collection

Experimental procedures involving mice were approved by the Animal Use Subcommittee of the University Council on Animal Care of the University of Western Ontario and were in accordance with the International Guiding Principles for Biomedical Research Involving Animals as promulgated by the Society for the Study of Reproduction. Three and 5 week old CD1 female mice (5 from each age group) were anesthetized with CO<sub>2</sub> and killed by cervical dislocation. The ovaries were removed and placed in McCoy's 5A complete medium containing 10% fetal bovine serum (FBS), 100 units/ml penicillin, and 100  $\mu$ g/ml streptomycin. All products for this study were purchased from Invitrogen Canada Inc. (Burlington, ON) unless otherwise specified. Surrounding fat and connective tissue were removed using 25-gauge needles. The ovaries were fixed in Bouin's solution overnight, embedded in paraffin and sectioned at 5  $\mu$ m.

### Culture of Granulosa Cells

Ovaries from 3 week old CD1 female mice were digested in McCoy's 5A complete medium containing 2 mg/ml type I collagenase (Sigma-Aldrich Canada Ltd., Oakville, Ontario) at 37°C for 10–15 minutes. Secondary and early tertiary (antral) follicles were liberated by repeated aspiration and expulsion with a 1 ml pipettor. Follicles and cumulus-oocyte complexes were washed with culture medium and transferred to another dish in which the oocytes were separated from the granulosa cells by treatment with 0.05% trypsin-EDTA for 5 minutes followed by centrifugation at 600 g for 5 minutes. The supernatant (containing oocytes) was removed and the granulosa cells resuspended in McCoy's 5A complete medium. Granulosa cells were cultured on 12 mm glass coverslips or in 6-well plates at 37°C, 5% CO<sub>2</sub> in air.

### Antibodies

All antibodies used in this study are commercially available and have been widely used and their specificity demonstrated in previous studies [16, 27–34]. They are listed in Table 1.

### Immunohistochemistry

Immunohistochemistry was performed using the Goat ABC Staining System (Santa Cruz Biotechnology Inc., Santa Cruz, CA). Briefly, the sections were deparaffinized completely and then immersed in citric acid buffer (10 mmol/L of sodium citrate, 10 mmol/L of citric acid) and boiled in a microwave oven at 92–98°C for 15 min to expose the antigens. The sections were cooled to room temperature and then sequentially incubated at room

temperature with 3% H<sub>2</sub>O<sub>2</sub> in methanol for 15 min to quench endogenous peroxidase; blocked with normal serum for 45 min; incubated in goat anti-WNT2 antibody (2.0 µg/ml, Santa Cruz) at 4°C overnight; incubated in biotinylated secondary antibody for 1 hr; and finally treated with the AB reagent for 1 h. Intervening PBS washes were performed after incubation when necessary. The sections were stained with diaminobenzidine (DAB) and mounted as described above. As a negative control, slides were incubated without primary antibody or with the WNT2 antibody plus WNT2 blocking peptide provided by Santa Cruz. The signals were recorded with a Leica digital camera system (Leica Microsystems Canada Inc., Richmond Hill, Ontario), and the digital images were processed by Adobe PhotoShop (Version 7.0; Adobe, San Jose, CA).

### siRNA Transfection and Recombinant Viral Infection

Several siRNAs were tested at different concentrations for each knockdown experiment with the results presented here being obtained from the single most effective siRNA. Granulosa cells to be used for siRNA transfection were changed into medium without antibiotics after 6 h and cultured for a further 48 h for transfection. Stealth™/siRNA duplex oligoribonucleotides for WNT2 and β-catenin were ordered from Invitrogen along with negative siRNA (lacking homology with any vertebrate sequence) as a toxicity control. Transfection was achieved using Lipofectamine™ RNAiMAX reagent using the recommended protocol. For WNT2 the best inhibitory effect was achieved with siRNA-3 (aca ccc aga ugu gau gcg ugc cau u) at 10 nM. For β-catenin, the best inhibitory effect was achieved with siRNA-2 (ccc aga aug ccg uuc gcc uuc auu a) at 100 nM. The respective negative siRNAs were used at the same concentrations.

The mouse WNT2 conventional vector was generously provided by Dr. Diana Klein (University of Heidelberg, Germany) [18]. The cDNA was released and inserted into the AP2 retroviral vector (a murine plasmid retrovector including the enhanced green fluorescent protein (EGFP) reporter gene) using restriction endonucleases BglII and BamHI. The inserted cDNA and EGFP coding fragments were connected by an internal ribosome entry site (IRES) to facilitate independent translation of the two proteins. The AP2 vector without any inserted fragment was used for the empty vector control. WNT2 vector or empty vector was transduced into 293 GPG packaging cells by transfection to produce infective virus which was then used to infect granulosa cells. Virus production from the WNT2 construct and the empty vector was similar as described previously [35]. Cells grown to 40–50% confluency were incubated with concentrated retrovirus (200 µl virus was added into 2 ml culture medium) for 40 hours at 37°C. Infection efficiency was determined 48 hours after infection by visualizing live or fixed cells for EGFP expression. Cells and medium were harvested after 48 hrs culture, but the medium was replaced and cells were cultured in FBS-free medium for a further 6–8 hrs before harvest. The medium protein was concentrated by Amicon® Ultra Centrifugal Filter Devices (Millipore, Billerica, MA) according to the company's protocol. Before sample collection, the cell morphology was recorded using a Leica digital camera system.

In experiments where siRNA treatment was combined with viral vector infection, the siRNA was diluted into medium containing infectious virus to obtain the appropriate reagent concentrations.

### Immunofluorescence Microscopy

Cells grown on glass coverslips were fixed with pre-chilled methanol/acetone (1:1) at  $-20^{\circ}\text{C}$  for 20 min or with 3.7% PFA (for cells expressing GFP) at  $4^{\circ}\text{C}$  for 15 min, and then rinsed with phosphate-buffered saline (PBS) and prepared for immunostaining as previously described [25]. Briefly, the cells were blocked with washing buffer containing 3% BSA (w/v) for 1 h, immunolabeled with primary antibody for 1 h, washed with PBS, and immunolabeled with appropriate secondary antibody for 1 h in the dark. Several washes were interposed between different antibody incubations. Cells were washed in PBS and the nuclei were stained with 0.1% Hoechst for 10 min followed by washes with PBS and double distilled  $\text{H}_2\text{O}$ . The coverslips were mounted on slides with Airvol before storage at  $4^{\circ}\text{C}$ . The cells were imaged using a Zeiss LSM 510 META confocal microscope. Fluorescent signals were captured after excitation with 488, 543, or 730 nm laser lines.

### Western Blotting

Whole cell proteins were extracted with lysis buffer containing 50 mmol/L Tris-HCl (pH 8.0), 150 mmol/L sodium chloride, 0.02% sodium azide, 1% NP-40, 0.1% SDS, 0.5% sodium deoxycholate, 2 mM NaF, 2 mM  $\text{Na}_3\text{VO}_4$ , and 1X protease inhibitor cocktail. To measure protein secreted into the medium, the medium was replaced with FBS-free medium for 6–8 hrs before harvest. The medium protein was concentrated by Amicon<sup>®</sup> Ultra Centrifugal Filter Devices (Millipore, Billerica, MA) according to the manufacturer's protocol. Twenty  $\mu\text{g}$  total protein for cells or 50  $\mu\text{g}$  total protein for concentrated medium were separated by SDS-polyacrylamide gel electrophoresis (SDS-PAGE) on 12% gels, and proteins were transferred to nitrocellulose membrane using iBlot Gel Transfer Stacks (Invitrogen). The membrane was blocked with 0.5% BSA (w/v) in TBST for 1 h, and subsequently probed with the corresponding primary antibody overnight at  $4^{\circ}\text{C}$  followed by incubation with infrared fluorescent-labeled secondary antibody (Alexa-680 anti-rabbit, anti-goat or anti-mouse). Antibody binding was detected by use of the Odyssey infrared-imaging system (LI-COR Biosciences, Lincoln, NE). The membrane was stripped and re-probed with other primary antibodies overnight at  $4^{\circ}\text{C}$  and followed by incubation with the corresponding infrared fluorescent-labeled secondary antibody. The immunoblots were processed using LI-COR. Two washes with TBST were inserted between the antibody treatment steps. The relative intensity of protein bands was determined in reference to glyceraldehyde phosphate dehydrogenase (GAPDH) and quantified using Quantity One software (Bio-Rad Laboratories (Canada) Ltd, Mississauga, ON).

### Proliferation Assay

Cell proliferation was measured using the Click-iT<sup>™</sup> EdU Imaging Kit from Invitrogen. After 48 hr culture with siRNA or viral vector, 20  $\mu\text{M}$  EdU was added to the medium and the cells allowed to grow for another 4–6 hrs before scoring them for EdU incorporation. Briefly, the cells were fixed with 3.7% PFA in PBS for 15 minutes and washed with 3% BSA twice, then incubated with 0.5% Triton<sup>™</sup> X-100 for 20 minutes, followed by

incubation with the Click-iT™ reaction cocktail for 30 minutes in the dark. The nuclei were stained with 0.1% Hoechst in PBS for 10 minutes. Intervening 3% BSA washes were performed after incubation when necessary. The coverslips were mounted on slides with Airvol. Fluorescent signals were captured after excitation with 488 and 730 nm laser lines. The ratio of EdU positive cells to the total number of cells was determined for each of 15–20 fields (4–5 fields per coverslip with 3–4 replicate coverslips per experiment).

### Apoptosis Assay

Apoptosis was detected using the DeadEnd™ Fluorometric TUNEL System (Promega, Madison, WI) according to the manufacturer's instructions. Briefly, the sections were deparaffinized completely and fixed in 3.7% paraformaldehyde (PFA) in PBS for 15 minutes at room temperature. The sections were treated with 20 µg/ml proteinase K for 8–10 minutes and fixed in 3.7% PFA for 5 minutes. For cell staining, the cells were first fixed in 3.7% PFA for 25 minutes at 4°C, washed with PBS and treated with 0.2% Triton™ X-100 for 5 minutes. The sections or cells were incubated in equilibration buffer for 10 minutes followed by rTdT incubation buffer at 37°C for 1 hr, and washed with 2× SSC and PBS, and mounted with Airvol (Air Products & Chemicals, Inc., Allentown, PA). The nuclei were stained with 0.1% Hoechst for 10 minutes before mounting. For the positive control, the section or cells were treated with 10 units/ml DNase I for 10 minutes before incubation with rTdT incubation buffer. The results were imaged using a Zeiss (Thornwood, NY) LSM 510 META confocal microscope. Fluorescent signals were captured after excitation with 488 nm laser lines. Digital images were prepared using Zeiss LSM and Adobe Photoshop 7.0 software. The ratio of TUNEL positive cells to the total number of cells was determined for each of 15–20 fields (4–5 fields per coverslip with 3–4 replicate coverslips per experiment).

### Statistical Analysis

Statistical analysis (one-way ANOVA with a post-hoc test when appropriate) was performed using the Statistical Package for Social Science (SPSS 13.0 for Windows; SPSS Inc., Chicago, IL). Data are presented as mean ± S.E. and  $P < 0.05$  was considered to be significant. In all graphical figures, different letters above bars indicate significant differences between treatments.

## RESULTS

### Expression of WNT2 in the Mouse Ovary and Its Relationship to Follicle Atresia

Previous work revealed that WNT2 mRNA is concentrated in the granulosa cells of rat ovary [23] and that WNT2 and members of the WNT signaling pathway are expressed in human cumulus cells [25]. In the present study, immunocytochemistry applied to ovary sections demonstrated that WNT2 is also expressed in mouse granulosa cells, both cumulus and mural (Figure 1). Immunofluorescence analysis of cultured granulosa cells revealed that it co-localizes with FZD3 and FZD9 (see Supplementary Data). Furthermore, in co-immunoprecipitation experiments, we found that WNT2 antibody could precipitate FZD3 and FZD9, but only FZD9 antibody could precipitate WNT2 suggesting that FZD9 may be the preferred receptor for WNT2 in mouse granulosa cells (Supplementary Data). WNT2 is expressed in the granulosa cells of all stages of follicles in 3-week-old mouse ovaries

(Figure 1). The signals were much stronger in the cumulus and mural granulosa cells of antral follicles, but not in all antral follicles (Fig. 1A, 3 weeks). In 5 week old ovary, WNT2 was detected in the granulosa cells and corpus luteum, but expression varied between different antral follicles (Fig. 1A, 5 weeks). To examine a possible association between WNT2 expression and follicle atresia, apoptosis was examined by TUNEL staining. WNT2 is highly expressed in the granulosa cells of healthy follicles (red arrows), but the signal strength was reduced in the granulosa cells of atretic (TUNEL-positive) follicles (yellow arrows) (Fig. 1D).

### **WNT2 Knockdown Inhibits DNA Synthesis in Granulosa Cells**

WNT2 level in both cells and medium was reduced by 70% or more with 10 nM siRNA-3 (Fig. 2A,B;  $P < 0.001$ ). To examine the effect of this treatment on proliferation, we monitored the incorporation into DNA of EdU (5-ethynyl-2'-deoxyuridine), an analog of thymidine, as a surrogate [36]. In normal and negative control siRNA-treated granulosa cells, the proportion of cells incorporating EdU was ~40% whereas it was as low as 10% in WNT2 siRNA-treated cells (Fig. 2C). To confirm this result, we also quantified proliferating cell nuclear antigen (PCNA), a marker for cells in S phase, by western blot. PCNA is an auxiliary protein of DNA polymerase  $\delta$  that is essential for DNA replication during S-phase [37, 38]. PCNA begins to accumulate during the G1 phase of the cell cycle, is most abundant during the S phase, and declines during the G2/M phase [39]. WNT2 siRNA significantly decreased the PCNA level compared to normal and negative siRNA-treated granulosa cells (Fig. 2D;  $P < 0.001$ ).

### **WNT2 Overexpression Promotes DNA synthesis in Granulosa Cells**

To further characterize the role of WNT2 in the proliferation of granulosa cells, we overexpressed it by infecting the cells with AP2 retroviral vector containing mWNT2 cDNA. The construct also included an enhanced green fluorescent protein (EGFP) cassette as a reporter downstream of an IRES (Fig. 3A). After 48 hrs infection, the expression level of WNT2 protein was detected by immunostaining and immunoblotting. We found that at least 60% of granulosa cells exposed to the vector exhibited GFP fluorescence, and the WNT2 immunofluorescent signal was higher in WNT2 overexpressing granulosa cells than in normal (uninfected) and empty vector infected cells (Fig. 3B). Western blotting revealed that WNT2 level in overexpressing cells and their culture medium was twice that of normal and empty vector infected cells (Fig. 3C;  $P < 0.05$  for the cells,  $P < 0.001$  for the medium). After 4 hrs incubation with 20 nM EdU, the proportion of positive (EdU incorporating) cells was significantly higher in WNT2 overexpressing cells (60% or more) than in normal and empty vector infected cells (less than 40%) (Fig. 3D;  $P < 0.001$ ). WNT2 overexpression also markedly increased PCNA expression compared to normal and empty vector-infected cells (Fig. 3E;  $P < 0.001$ ).

### **WNT2 Regulates GSK-3 $\beta$ and $\beta$ -Catenin Expression and $\beta$ -Catenin Localization in Granulosa Cells**

The protein kinase GSK-3 $\beta$  an important component of the  $\beta$ -catenin destruction complex, regulates the phosphorylation of  $\beta$ -catenin [40]. The level of GSK-3 $\beta$  was altered by treatments that increased or decreased WNT2. In normal granulosa cells, GSK-3 $\beta$  is mostly

localized in the cytoplasm (see Fig. 4A). WNT2 siRNA knockdown increased the GSK-3 $\beta$  immunofluorescent signal in the cytoplasm and significantly increased its total protein level as revealed by western blotting (Fig. 4A,B;  $P < 0.05$ ). In contrast, WNT2 overexpression significantly reduced the accumulation of GSK-3 $\beta$  (Fig 4C,D;  $P < 0.05$ ). In both cases, the negative control treatment had no effect.

We next focused our attention on  $\beta$ -catenin, the central player in the WNT canonical pathway by virtue of its role as a transcription cofactor that activates gene expression to regulate cell proliferation and differentiation [41].  $\beta$ -catenin is also a structural adaptor protein linking cadherins to the actin cytoskeleton in cell-cell adhesion [42]. Consistent with our previous results with human cumulus cells [25],  $\beta$ -catenin was mostly localized in the membranes of normal and negative siRNA-treated granulosa cells (Fig. 6, see yellow arrows) with additional weak staining in the cytoplasm and nucleus (Fig. 5A). In WNT2 siRNA-treated cells,  $\beta$ -catenin expression in the membranes was markedly reduced, and the total  $\beta$ -catenin level was also significantly decreased (Fig. 5A,B;  $P < 0.001$ ). In contrast, WNT2 overexpression significantly increased total  $\beta$ -catenin level ( $P < 0.05$ ) but altered its distribution:  $\beta$ -catenin in the membranes was reduced leaving most of the immunofluorescent signal in the nucleus and cytoplasm (Fig. 5C,D; see white arrows).

### **$\beta$ -Catenin Knockdown Inhibits DNA synthesis in Granulosa Cells and Blunts the Stimulatory Effect of WNT2**

Our recent work with human cumulus cells indicated that WNT2 acts through its receptor FZD9 to regulate the formation of adherens junctions involving  $\beta$ -catenin and E-cadherin [25]. In cells treated with  $\beta$ -catenin siRNA,  $\beta$ -catenin immunofluorescence was rarely detected in the membranes and other compartments of the treated cells, and its level was reduced to as low as 20% of that in normal or negative siRNA-treated cells (Fig. 6A,B).  $\beta$ -catenin siRNA also reduced the proportion of cells in S phase to as low as 10% while normal and negative siRNA-treated cells showed on average 60% positive cells after 6 hrs incubation with EdU (Fig. 6C). PCNA expression was significantly inhibited by  $\beta$ -catenin siRNA (Fig. 6D;  $P < 0.001$ ).  $\beta$ -catenin knockdown did not affect WNT2 expression (data not shown).

To test the hypothesis that WNT2 regulates the proliferation of granulosa cells via  $\beta$ -catenin, granulosa cells were treated with WNT2 overexpression vector and  $\beta$ -catenin siRNA together. After 4 hrs incubation, the proportion of EdU positive cells was close to 40% in normal and empty vector-treated cells but it was increased to 70% in WNT2 overexpressing cells ( $P < 0.001$ ).  $\beta$ -catenin siRNA knockdown decreased the proportion of cells in S phase to as low as 20% ( $P < 0.001$ ) and there was no significant difference between cells treated with  $\beta$ -catenin siRNA alone, cells treated with empty vector plus  $\beta$ -catenin siRNA, and cells treated with WNT2 vector plus  $\beta$ -catenin siRNA (Fig. 7A). These results were confirmed by PCNA immunoblotting:  $\beta$ -catenin siRNA alone decreased the PCNA level ( $P < 0.001$ ), but WNT2 vector significantly increased the PCNA level ( $P < 0.001$ ) and that increase was neutralized by  $\beta$ -catenin siRNA (Fig. 7B;  $P > 0.05$  compared with normal cells). Finally, to test the hypothesis that WNT2/ $\beta$ -catenin signaling influences granulosa cell proliferation via an effect on cyclin expression, we measured the level of cyclin D2, the predominant cyclin



isoform in granulosa cells [44], after  $\beta$ -catenin knockdown and WNT2 overexpression. As shown in Fig. 7C,  $\beta$ -catenin knockdown significantly reduced cyclin D2 expression whereas WNT2 overexpression significantly increased it.

### WNT2/ $\beta$ -Catenin Signaling Influences Apoptosis of Granulosa Cells

WNT/ $\beta$ -catenin signaling can regulate programmed cell death, for example in malignant melanoma and colorectal cancer cells where inhibition of WNT2 induced apoptosis [44, 45]. In our study, we found that WNT2 siRNA significantly increased the frequency of apoptosis (18% of granulosa cells,  $P < 0.05$ ) compared with normal or negative siRNA-treated cells in which apoptotic cells were rarely found (Fig. 8A,B). Cells treated with  $\beta$ -catenin siRNA also trended toward a greater frequency of apoptosis but the difference just missed significance ( $P = 0.058$ ). WNT2 overexpression had no effect on apoptosis (WNT2 vector vs. empty vector,  $P > 0.05$ ).

## DISCUSSION

WNTs and their receptors orchestrate many essential cellular and physiological processes. During development they control cell proliferation, differentiation, migration, and patterning [46]. Canonical WNT signaling causes  $\beta$ -catenin accumulation in the nucleus in a complex with the transcription factor TCF/LEF that regulates target gene expression [2, 47]. In our recent study [25], WNT2 and several members of the canonical WNT pathway, including FZD9 and  $\beta$ -catenin, were identified and shown to interact in human cumulus granulosa cells. It was thus our objective in the present study to explore the function and regulation of WNT2 signaling in mouse granulosa cells.

Ovarian follicle development occurs in several stages including primordial follicle recruitment, oocyte growth, follicle growth through granulosa cell proliferation, and follicle demise through atresia (apoptosis) of granulosa and theca cells leaving only one or a few follicles to reach the ovulatory stage in each cycle, depending on the species [48]. In previous work, WNT2 mRNA was observed in the granulosa cells of rat follicles at all stages of development, but appeared to be more intense in large preantral and antral follicles [23]. Consistent with this, in the present study WNT2 was found in the granulosa cells of all stages of follicle in 3 week old mice (when few growing follicles have reached the preovulatory stage), with intense expression in the granulosa cells of antral follicles. In 5 week ovaries, the distribution of WNT2 was similar to that in 3 week ovaries except that it was also detected in the corpora lutea, where signal strength was much lower. That the strongest WNT2 signal was found in the granulosa cells of 3 week antral follicles implies that WNT2 plays an important role in folliculogenesis between the preantral and preovulatory stages. Interestingly, the strength of WNT2 expression appeared to vary between different antral follicles and was inversely associated with follicle atresia as indicated by TUNEL assay. Thus WNT2 may be involved in promoting antral follicle development and inhibiting follicle atresia. Although expressed in the corpus luteum, there is as yet no information supporting a role for WNT2 in that structure.

There is evidence that misregulation of WNT signaling is involved in ovarian tumorigenesis [26]. However, research has only recently begun to elucidate the function of the WNT/ $\beta$ -

catenin pathway in normal granulosa cells. In our study, WNT2 expression was successfully knocked down by WNT2 siRNA, inhibiting DNA synthesis as revealed both by the EdU incorporation assay and by measuring PCNA. The fact that WNT2 siRNA reduced PCNA expression in granulosa cells implies that WNT2 knockdown disrupted the granulosa cell cycle during the G1 and S phases. To further confirm this conclusion, WNT2 was overexpressed in granulosa cells by infection with a WNT2-encoding retroviral vector. Both the proportion of EdU positive cells and the expression of PCNA were up-regulated by WNT2 overexpression. Thus WNT2 has the ability to enhance the accumulation of PCNA and accelerate DNA synthesis, presumably promoting the proliferation of granulosa cells. Since  $\beta$ -catenin knockdown reduced cyclin D2 level (Fig. 7), it is likely that the influence of WNT2/ $\beta$ -catenin signaling on granulosa cell proliferation is mediated, at least in part, by this cell cycle regulator; indeed, cyclin D2 knockout females are infertile, with the primary cause being failure of the granulosa cells to proliferate in response to FSH (49). However, there must be other signaling molecules, including perhaps other members of the WNT family, involved in stimulating granulosa cell proliferation that can compensate for reduced WNT2 activity since *Wnt2* null female mice were reported to be fertile [14]. Unfortunately, there are no published data on ovulation rate or litter size in *Wnt2* null females that might indicate a reduction in oocyte production without loss of fertility.

At the heart of the canonical WNT signaling pathway is the  $\beta$ -catenin destruction complex, which is composed of CK1 $\alpha$ , AXIN, GSK-3 $\beta$ , and APC and determines the fate of  $\beta$ -catenin in the cells [5, 6, 50]. However, the mechanism of  $\beta$ -catenin regulation by the destruction complex is not clearly understood. In WNT2 siRNA-treated granulosa cells, more GSK-3 $\beta$  accumulated in the cytoplasm and  $\beta$ -catenin was reduced. Increasing expression of GSK-3 $\beta$  enhances  $\beta$ -catenin phosphorylation, and phosphorylated  $\beta$ -catenin is marked for rapid ubiquitinylation and degradation via the proteasome [5]. In contrast, overexpression of WNT2 decreased GSK-3 $\beta$  in the cytoplasm, allowing more  $\beta$ -catenin to accumulate in the nucleus. Low GSK-3 $\beta$  results in inhibition of  $\beta$ -catenin phosphorylation, allowing dephosphorylated  $\beta$ -catenin to accumulate, enter the nucleus, and activate WNT target gene expression [6]. The nuclear level of  $\beta$ -catenin has been found to correlate better with WNT activity [51]. Thus WNT2 overexpression could change the distribution of  $\beta$ -catenin from the membrane into the nucleus, activating  $\beta$ -catenin signaling.

It has been found that WNT/ $\beta$ -catenin positively regulates progenitor proliferation by promoting G1 to S progression [13]. In the present study, very few proliferating cells were found in  $\beta$ -catenin siRNA-treated cultures, and  $\beta$ -catenin siRNA markedly decreased PCNA expression. This indicates that  $\beta$ -catenin knockdown reduced cell proliferation by inhibiting the cell cycle at the G1 to S transition, which is consistent with the results from the WNT2 siRNA experiments. Most importantly,  $\beta$ -catenin siRNA neutralized the ability of WNT2 overexpression to enhance proliferation. Therefore, we conclude that WNT2 stimulates the proliferation of granulosa cells through the activation of  $\beta$ -catenin. This interpretation of the pivotal role of  $\beta$ -catenin in WNT2 stimulation of follicle growth is all the more interesting in light of the recent results of Hernandez Gifford et al. [52], who demonstrated that  $\beta$ -catenin is also required for FSH-stimulated estradiol production by granulosa cells. These two findings, taken together, suggest that WNT and FSH signaling pathways in granulosa cells

intersect at  $\beta$ -catenin. The relationship between the WNT and FSH signaling pathways in growing follicles merits further investigation.

Although it is well accepted that WNT2 influences apoptosis of cancer cells [44, 45], this has not been confirmed in normal cells. We found that WNT2 siRNA knockdown could only induce apoptosis in a small minority of granulosa cells. Thus knockdown of WNT2 signaling reduces the proliferation of granulosa cells primarily by slowing down the cell cycle, not by inducing apoptosis.

In conclusion, our results make it clear that the canonical WNT signaling pathway is intact in mouse granulosa cells and that WNT2 can act through  $\beta$ -catenin, likely downstream of FZD9, to regulate their proliferation. Future experiments must be directed to determining whether WNT2 acts downstream of FSH to influence steroidogenesis, or if, conversely, the WNT2/ $\beta$ -catenin and FSH signaling cascades operate in parallel. In either case, the canonical WNT pathway should be considered a possible contributor to female fertility.

## Acknowledgments

We thank Dr. Diana Klein of the University of Heidelberg, Germany for providing the mWNT2 plasmid. We gratefully acknowledge the technical advice and assistance of Dr. Dan Tong and Kevin Barr.

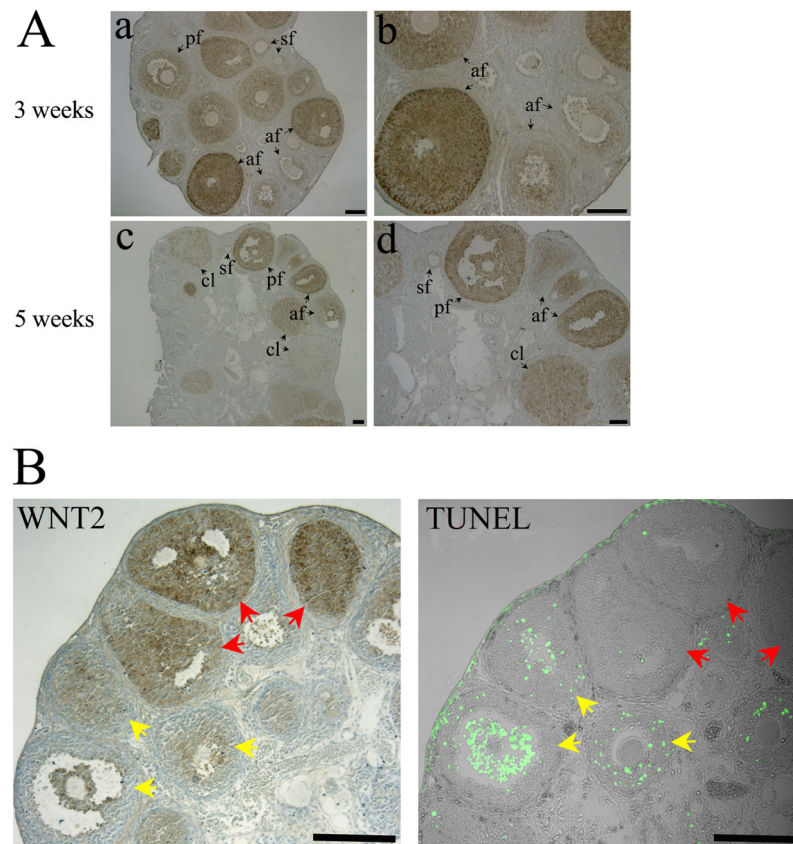
## References

1. Logan CY, Nusse R. The Wnt signaling pathway in development and disease. *Annu Rev Cell Dev Biol.* 2004; 20:781–810. [PubMed: 15473860]
2. Hoppler S, Kavanagh CL. Wnt signalling: variety at the core. *J Cell Sci.* 2007; 120:385–393. [PubMed: 17251379]
3. Clevers H. Wnt/beta-catenin signaling in development and disease. *Cell.* 2006; 127:469–480. [PubMed: 17081971]
4. Komiya Y, Habas R. Wnt signal transduction pathways. *Organogenesis.* 2008; 4:68–75. [PubMed: 19279717]
5. Kimelman D, Xu W. beta-catenin destruction complex: insights and questions from a structural perspective. *Oncogene.* 2006; 25:7482–7491. [PubMed: 17143292]
6. Lee E, Salic A, Krüger R, Heinrich R, Kirschner MW. The roles of APC and Axin derived from experimental and theoretical analysis of the Wnt pathway. *PLoS Biol.* 2003; 1:E10. [PubMed: 14551908]
7. Gordon MD, Nusse R. Wnt signaling: multiple pathways, multiple receptors, and multiple transcription factors. *J Biol Chem.* 2006; 281:22429–22433. [PubMed: 16793760]
8. Ulloa F, Briscoe J. Morphogens and the control of cell proliferation and patterning in the spinal cord. *Cell Cycle.* 2007; 6:2640–2649. [PubMed: 17912034]
9. Ikeya M, Lee SM, Johnson JE, McMahon AP, Takada S. Wnt signalling required for expansion of neural crest and CNS progenitors. *Nature.* 1997; 389:966–970. [PubMed: 9353119]
10. Muroyama Y, Fujihara M, Ikeya M, Kondoh H, Takada S. Wnt signaling plays an essential role in neuronal specification of the dorsal spinal cord. *Genes Dev.* 2002; 16:548–553. [PubMed: 11877374]
11. Yamaguchi TP, Bradley A, McMahon AP, Jones SA. Wnt5a pathway underlies outgrowth of multiple structures in the vertebrate embryo. *Development.* 1999; 126:1211–1223. [PubMed: 10021340]
12. Shu W, Jiang YQ, Lu MM, Morrissey EE. Wnt7b regulates mesenchymal proliferation and vascular development in the lung. *Development.* 2002; 129:4831–4842. [PubMed: 12361974]

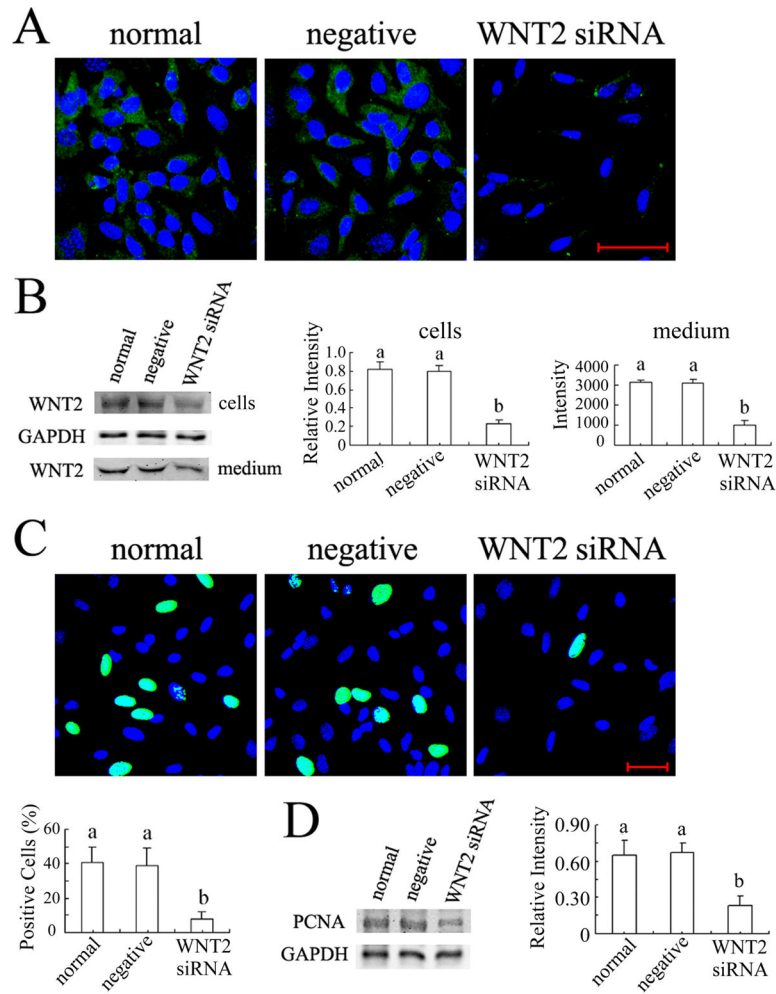
13. Zechner D, Fujita Y, Hülsken J, Müller T, Walther I, Taketo MM, Crenshaw EB 3rd, Birchmeier W, Birchmeier C. Beta-catenin signals regulate cell growth and the balance between progenitor cell expansion and differentiation in the nervous system. *Dev Biol.* 2003; 258:406–418. [PubMed: 12798297]
14. Monkley SJ, Delaney SJ, Pennisi DJ, Christiansen JH, Wainwright BJ. Targeted disruption of the *Wnt2* gene results in placentation defects. *Development.* 1996; 122:3343–3353. [PubMed: 8951051]
15. Katoh M. Frequent up-regulation of WNT2 in primary gastric cancer and colorectal cancer. *Int J Oncol.* 2001; 19:1003–1007. [PubMed: 11605001]
16. You L, He B, Xu Z, Uematsu K, Mazieres J, Fujii N, Mikami I, Reguart N, McIntosh JK, Kashani-Sabet M, McCormick F, Jablons DM. An anti-Wnt-2 monoclonal antibody induces apoptosis in malignant melanoma cells and inhibits tumor growth. *Cancer Res.* 2004; 64:5385–5389. [PubMed: 15289346]
17. Mazieres J, You L, He B, Xu Z, Twogood S, Lee AY, Reguart N, Batra S, Mikami I, Jablons DM. Wnt2 as a new therapeutic target in malignant pleural mesothelioma. *Int J Cancer.* 2005; 117:326–332. [PubMed: 15900580]
18. Klein D, Demory A, Peyre F, Kroll J, Augustin HG, Helfrich W, Kzhyshkowska J, Schledzewski K, Arnold B, Goerd S. Wnt2 acts as a cell type-specific, autocrine growth factor in rat hepatic sinusoidal endothelial cells cross-stimulating the VEGF pathway. *Hepatology.* 2008; 47:1018–1031. [PubMed: 18302287]
19. Richards JS. Hormonal control of gene expression in the ovary. *Endocr Rev.* 1994; 15:725–751. [PubMed: 7705279]
20. Quirk SM, Cowan RG, Harman RM, Hu CL, Porter DA. Ovarian follicular growth and atresia: the relationship between cell proliferation and survival. *J Anim Sci.* 2004; 82:E40–E52. [PubMed: 15471814]
21. Vainio S, Heikkilä M, Kispert A, Chin N, McMahon AP. Female development in mammals is regulated by Wnt-4 signalling. *Nature.* 1999; 397:405–409. [PubMed: 9989404]
22. Hsieh M, Boerboom D, Shimada M, Lo Y, Parlow AF, Luhmann UF, Berger W, Richards JS. Mice null for Frizzled4 (*Fzd4*<sup>-/-</sup>) are infertile and exhibit impaired corpora lutea formation and function. *Biol Reprod.* 2005; 73:1135–1146. [PubMed: 16093361]
23. Ricken A, Lochhead P, Kontogiannia M, Farookhi R. Wnt signaling in the ovary: identification and compartmentalized expression of wnt-2, wnt-2b, and frizzled-4 mRNAs. *Endocrinology.* 2002; 143:2741–2749. [PubMed: 12072409]
24. Hsieh M, Johnson MA, Greenberg NM, Richards JS. Regulated expression of Wnts and Frizzleds at specific stages of follicular development in the rodent ovary. *Endocrinology.* 2002; 143:898–908. [PubMed: 11861511]
25. Wang HX, Tekpetey FR, Kidder GM. Identification of WNT/beta-CATENIN signaling pathway components in human cumulus cells. *Mol Hum Reprod.* 2009; 15:11–17. [PubMed: 19038973]
26. Boerboom D, Paquet M, Hsieh M, Liu J, Jamin SP, Behringer RR, Sirois J, Taketo MM, Richards JS. Misregulated Wnt/beta-catenin signaling leads to ovarian granulosa cell tumor development. *Cancer Res.* 2005; 65:9206–9215. [PubMed: 16230381]
27. Kashani-Sabet M, Rangel J, Torabian S, Nosrati M, Simko J, Jablons DM, Moore DH, Haqq C, Miller JR 3rd, Sagebiel RW. A multi-marker assay to distinguish malignant melanomas from benign nevi. *Proc Natl Acad Sci USA.* 2009; 106:6268–6272. [PubMed: 19332774]
28. Fujise T, Iwakiri R, Kakimoto T, Shiraishi R, Sakata Y, Wu B, Tsunada S, Ootani A, Fujimoto K. Long-term feeding of various fat diets modulates azoxymethane-induced colon carcinogenesis through Wnt/beta-catenin signaling in rats. *Am J Physiol Gastrointest Liver Physiol.* 2007; 292:G1150–1156. [PubMed: 17194898]
29. Macias E, Miliani de Marval PL, Senderowicz A, Cullen J, Rodriguez-Puebla ML. Expression of CDK4 or CDK2 in mouse oral cavity is retained in adult pituitary with distinct effects on tumorigenesis. *Cancer Res.* 2008; 68:162–171. [PubMed: 18172308]
30. Nunes RO, Schmidt M, Dueck G, Baarsma H, Halayko AJ, Kerstjens HA, Meurs H, Gosens R. GSK-3/beta-catenin signaling axis in airway smooth muscle: role in mitogenic signaling. *Am J Physiol Lung Cell Mol Physiol.* 2008; 294:L1110–1118. [PubMed: 18390827]

31. Petit-Paitel A, Brau F, Cazareth J, Chabry J. Involvement of cytosolic and mitochondrial GSK-3beta in mitochondrial dysfunction and neuronal cell death of MPTP/MPP-treated neurons. *PLoS ONE*. 2009; 4:e5491. [PubMed: 19430525]
32. Ligon LA, Karki S, Tokito M, Holzbaur EL. Dynein binds to beta-catenin and may tether microtubules at adherens junctions. *Nat Cell Biol*. 2001; 3:913–917. [PubMed: 11584273]
33. Rao RK, Basuroy S, Rao VU, Karnaky KJ Jr, Gupta A. Tyrosine phosphorylation and dissociation of occludin-ZO-1 and E-cadherin-beta-catenin complexes from the cytoskeleton by oxidative stress. *Biochem J*. 2002; 368:471–481. [PubMed: 12169098]
34. Yankiwski V, Marciniak RA, Guarente L, Neff NF. Nuclear structure in normal and Bloom syndrome cells. *Proc Natl Acad Sci USA*. 2000; 97:5214–5219. [PubMed: 10779560]
35. Tong D, Li TY, Naus KE, Bai D, Kidder GM. In vivo analysis of undocked connexin43 gap junction hemichannels in ovarian granulosa cells. *J Cell Sci*. 2007; 120:4016–4024. [PubMed: 17971414]
36. Wang Q, Chan TR, Hilgraf R, Fokin VV, Sharpless KB, Finn MG. Bioconjugation by copper (I)-catalyzed azide-alkyne [3+2] cycloaddition. *J Am Chem Soc*. 2003; 125:3192–3193. [PubMed: 12630856]
37. Harrison RF, Reynolds GM, Rowlands DC. Immunohistochemical evidence for the expression of proliferating cell nuclear antigen (PCNA) by non-proliferating hepatocytes adjacent to metastatic tumours and in inflammatory conditions. *J Pathol*. 1993; 171:115–122. [PubMed: 7904308]
38. Naryzhny SN. Proliferating cell nuclear antigen: a proteomics view. *Cell Mol Life Sci*. 2008; 65:3789–3808. [PubMed: 18726183]
39. Moldovan GL, Pfander B, Jentsch S. PCNA, the maestro of the replication fork. *Cell*. 2007; 129:665–679. [PubMed: 17512402]
40. Hedgepeth CM, Deardorff MA, Rankin K, Klein PS. Regulation of glycogen synthase kinase 3beta and downstream Wnt signaling by axin. *Mol Cell Biol*. 1999; 19:7147–7157. [PubMed: 10490650]
41. Nelson WJ, Nusse R. Convergence of Wnt, beta-catenin, and cadherin pathways. *Science*. 2004; 303:1483–1487. [PubMed: 15001769]
42. Jamora C, Fuchs E. Intercellular adhesion, signalling and the cytoskeleton. *Nat Cell Biol*. 2002; 4:E101–E108. [PubMed: 11944044]
43. Cannon JD, Cherian-Shaw M, Lovekamp-Swan T, Chaffin CL. Granulosa cell expression of G1/S phase cyclins and cyclin-dependent kinases in PMSG-induced follicle growth. *Mol Cell Endocrinol*. 2007; 264:6–15. [PubMed: 17084963]
44. You L, He B, Xu Z, Uematsu K, Mazieres J, Mikami I, Reguart N, Moody TW, Kitajewski J, McCormick F, Jablons DM. Inhibition of Wnt-2-mediated signaling induces programmed cell death in non-small-cell lung cancer cells. *Oncogene*. 2004; 23:6170–6174. [PubMed: 15208662]
45. Shi Y, He B, Kuchenbecker KM, You L, Xu Z, Mikami I, Yagui-Beltran A, Clement G, Lin YC, Okamoto J, Bravo DT, Jablons DM. Inhibition of Wnt-2 and galectin-3 synergistically destabilizes beta-catenin and induces apoptosis in human colorectal cancer cells. *Int J Cancer*. 2007; 121:1175–1181. [PubMed: 17534895]
46. Schlessinger K, Hall A, Tolwinski N. Wnt signaling pathways meet Rho GTPases. *Genes Dev*. 2009; 23:265–277. [PubMed: 19204114]
47. Wodarz A, Nusse R. Mechanisms of Wnt signaling in development. *Annu Rev Cell Dev Biol*. 1998; 14:59–88. [PubMed: 9891778]
48. Oktem O, Oktay K. The ovary: anatomy and function throughout human life. *Ann N Y Acad Sci*. 2008; 1127:1–9. [PubMed: 18443323]
49. Sicinski P, Donaher JL, Geng Y, Parker SB, Gardner H, Park MY, Robker RL, Richards JS, McGinnis LK, Biggers JD, Eppig JJ, Bronson RT, Elledge SJ, Weinberg RA. Cyclin D2 is an FSH-responsive gene involved in gonadal cell proliferation and oncogenesis. *Nature*. 1996; 384:470–474. [PubMed: 8945475]
50. Schwarz-Romond T, Metcalfe C, Bienz M. Dynamic recruitment of axin by Dishevelled protein assemblies. *J Cell Sci*. 2007; 120:2402–2412. [PubMed: 17606995]
51. Staal FJ, Noort Mv M, Strous GJ, Clevers HC. Wnt signals are transmitted through N-terminally dephosphorylated beta-catenin. *EMBO*. 2002; Rep 3:63–68.

52. Hernandez Gifford JA, Hunzicker-Dunn ME, Nilson JH. Conditional deletion of beta-catenin mediated by *Amhr2cre* in mice causes female infertility. *Biol Reprod.* 2009; 80:1282–1292. [PubMed: 19176883]

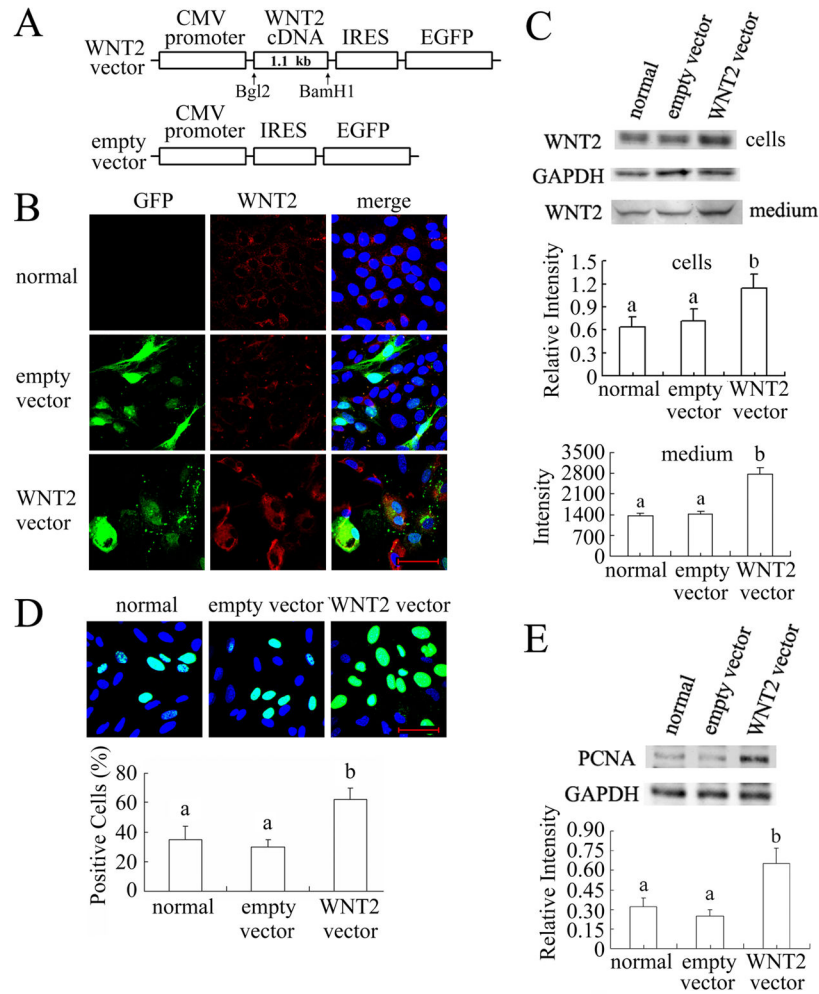


**FIG. 1.** Expression of WNT2 in mouse ovary and its relationship to follicle atresia. (A) Expression of WNT2 in ovaries of mice 3 and 5 weeks old (af, antral follicle; pf, preovulatory follicle; sf, small follicle; cl, corpus luteum). Scale bars = 100  $\mu$ m. Parts b and d are higher magnification images of a and c. (B) Inverse relationship between WNT2 expression (immunohistochemistry) and follicle atresia (TUNEL assay). Red arrows indicate healthy follicles, yellow arrows indicate atretic follicles.

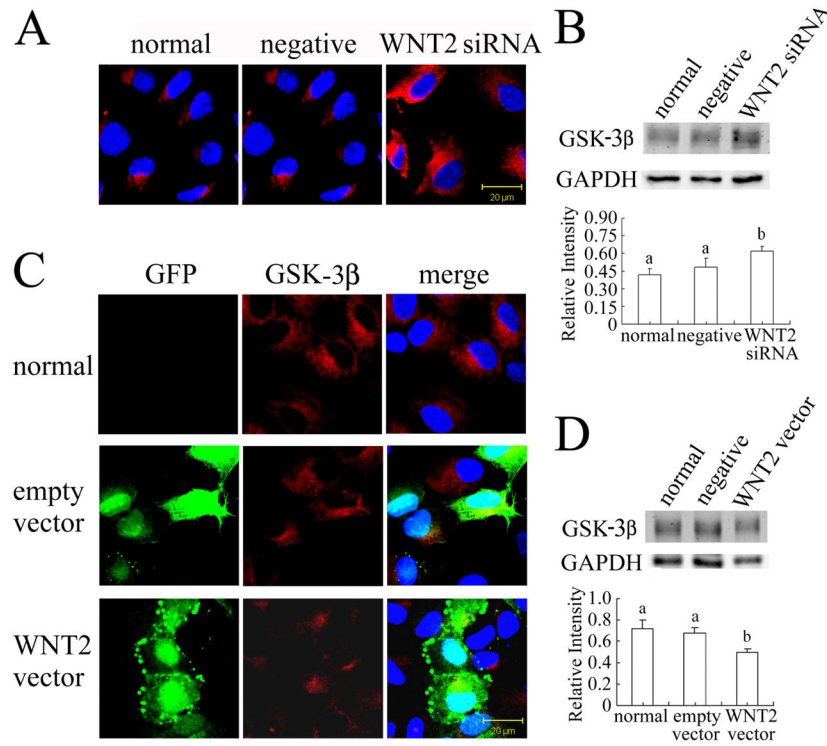


**FIG. 2.** WNT2 knockdown inhibited DNA synthesis in granulosa cells. (A) *Wnt2* mRNA knockdown reduced WNT2 immunostain (green fluorescence; nuclei labeled blue with Hoechst). (B) Quantification of WNT2 knockdown in the cells and medium by western blotting. The relative intensity of the WNT2 band in the cells was determined with respect to GAPDH but the band intensity in concentrated medium was quantified from 50  $\mu$ g total protein. (C) The proportion of granulosa cells incorporating EdU (green fluorescence) was significantly reduced by WNT2 siRNA knockdown (nuclei labeled with Hoechst). (D) PCNA level was also markedly reduced by WNT2 siRNA. Scale bars = 50  $\mu$ m.

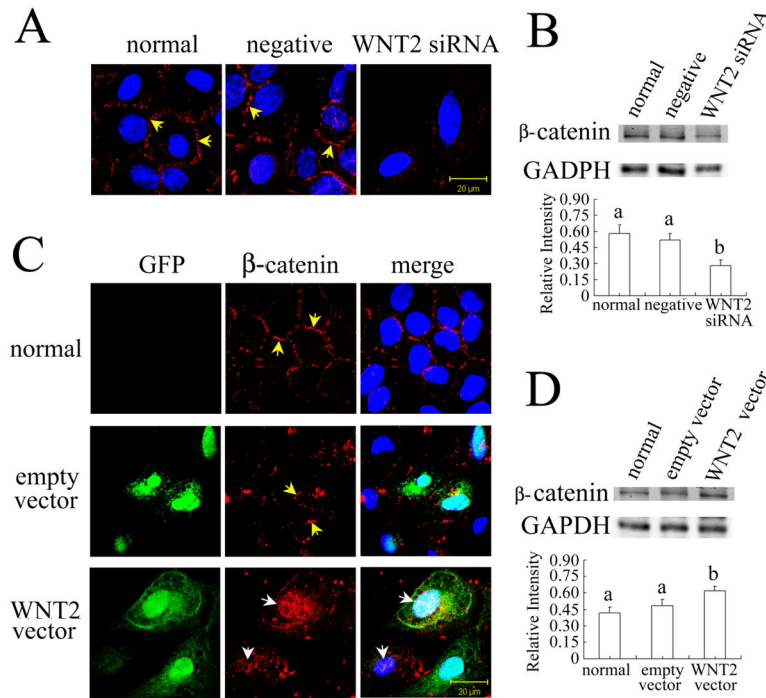




**FIG. 3.** WNT2 overexpression increased DNA synthesis in granulosa cells. (A) Maps of the mWNT2 overexpression retroviral vector and empty vector control (not to scale). A 1.1 kb mWNT2 cDNA was inserted into the AP2 vector using Bgl2 and BamHI; an EGFP cassette was added downstream, separated from the cDNA by an internal ribosome entry site (IRES). The empty vector control had the same structure except for the absence of WNT2 cDNA. (B,C) Overexpression of WNT2 in granulosa cells. After 48 hrs infection, the effect of WNT2 overexpression was detected by immunostaining (B) and immunoblotting (C) with WNT2 being quantified in the cells and concentrated medium as in Fig. 2B. (D) The proportion of cells incorporating EdU was significantly increased by WNT2 overexpression. (E) WNT2 overexpression markedly increased PCNA level. Scale bars = 50  $\mu$ m.

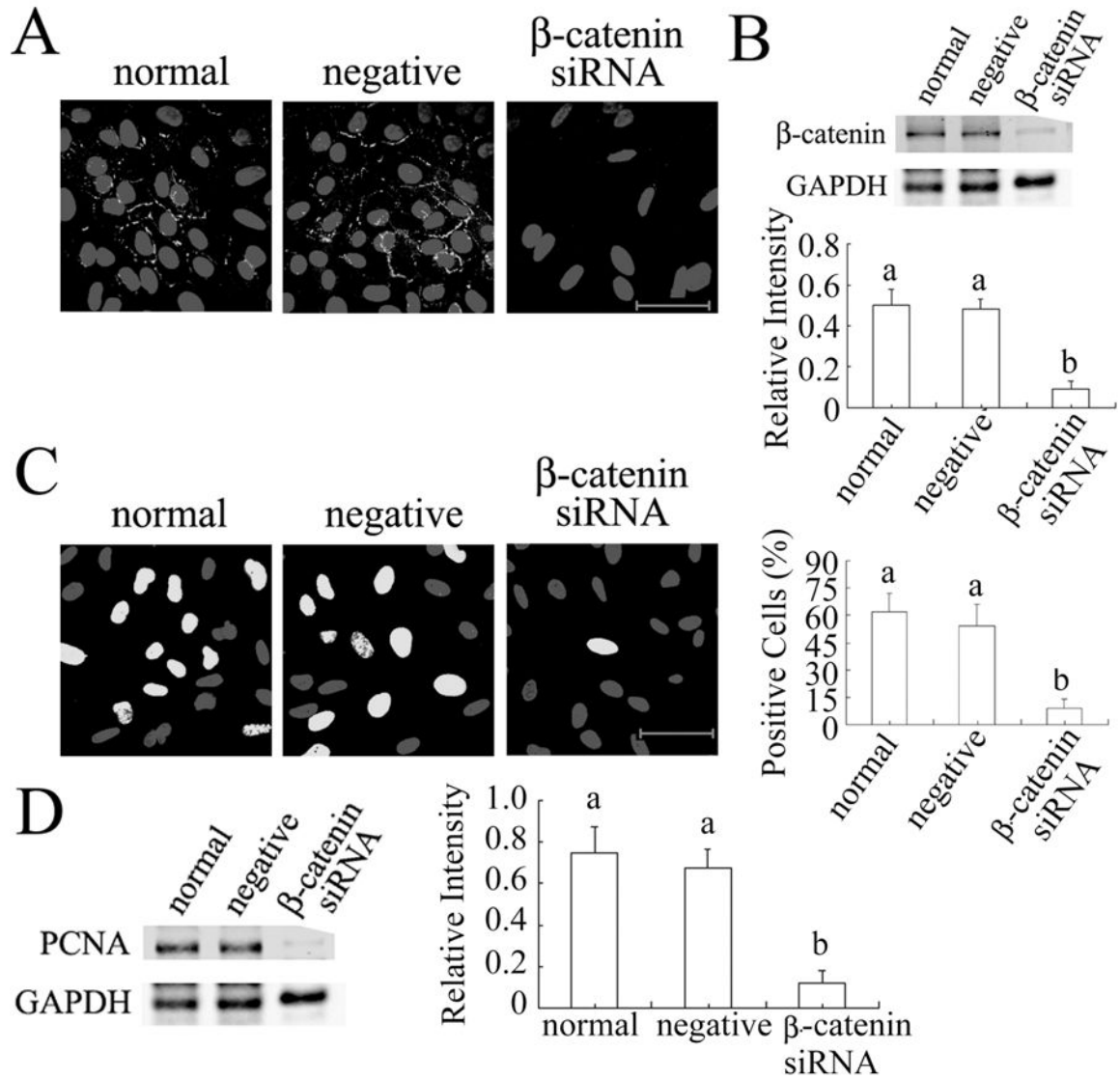


**FIG 4.** WNT2 regulates GSK-3 $\beta$  expression in granulosa cells. (A) WNT2 siRNA knockdown increased the GSK-3 $\beta$  immunofluorescent signal in the cytoplasm of granulosa cells. (B) GSK-3 $\beta$  level was significantly increased by WNT2 siRNA. (C) WNT2 overexpression reduced the GSK-3 $\beta$  immunofluorescent signal and (D) significantly reduced its level in granulosa cells. Scale bars = 20  $\mu$ m.

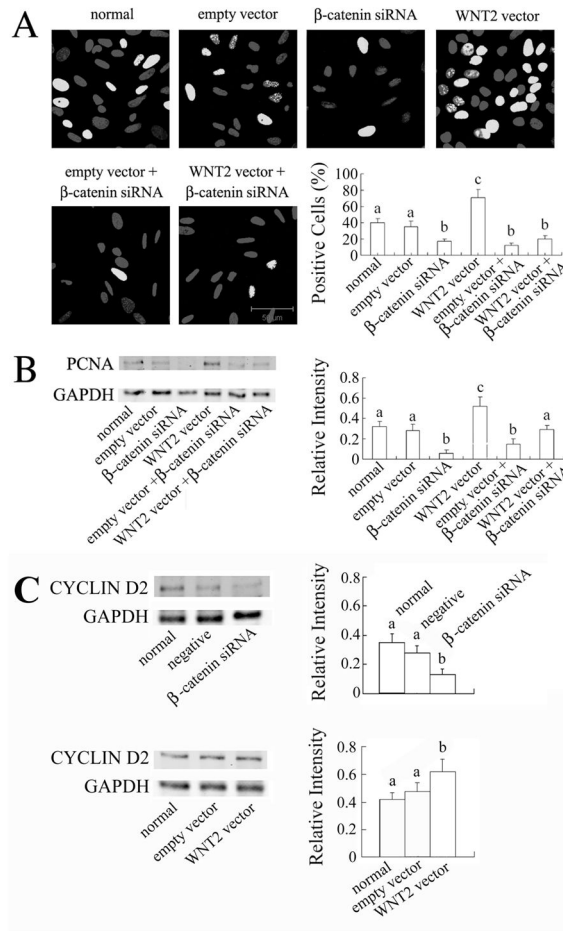
**FIG 5.**

WNT2 regulates  $\beta$ -catenin expression and localization in granulosa cells

(immunofluorescence detection of active  $\beta$ -catenin). (A) WNT2 siRNA knockdown inhibited the assembly of  $\beta$ -catenin into membranes (yellow arrows; scale bar = 20  $\mu$ m). (B) WNT2 siRNA significantly decreased  $\beta$ -catenin level. (C) WNT2 overexpression altered  $\beta$ -catenin localization from being primarily localized in the membranes of normal or empty vector-infected granulosa cells (yellow arrows) to being primarily in the nuclei of WNT2 overexpressing cells (white arrows). (D)  $\beta$ -catenin level was significantly increased by WNT2 overexpression.



**FIG. 6.**  $\beta$ -catenin knockdown inhibits DNA synthesis in granulosa cells. (A)  $\beta$ -catenin immunofluorescent signal was strongly reduced by its siRNA. (B)  $\beta$ -catenin was significantly reduced by its siRNA. (C)  $\beta$ -catenin siRNA significantly reduced the proportion of cells incorporating EdU. (D) PCNA level was significantly reduced by  $\beta$ -catenin siRNA. Scale bars = 50  $\mu$ m.

**FIG. 7.**

$\beta$ -catenin knockdown blunts the stimulatory effect of WNT2 overexpression on granulosa cell proliferation. (A)  $\beta$ -catenin siRNA reduced the proportion of cells incorporating EdU in the absence and presence of WNT2 vector. Scale bar = 50  $\mu$ m. (B)  $\beta$ -catenin siRNA reduced PCNA level in WNT2 vector-treated cells. (C)  $\beta$ -catenin siRNA also reduced cyclin D2 level, but WNT2 vector increased it.

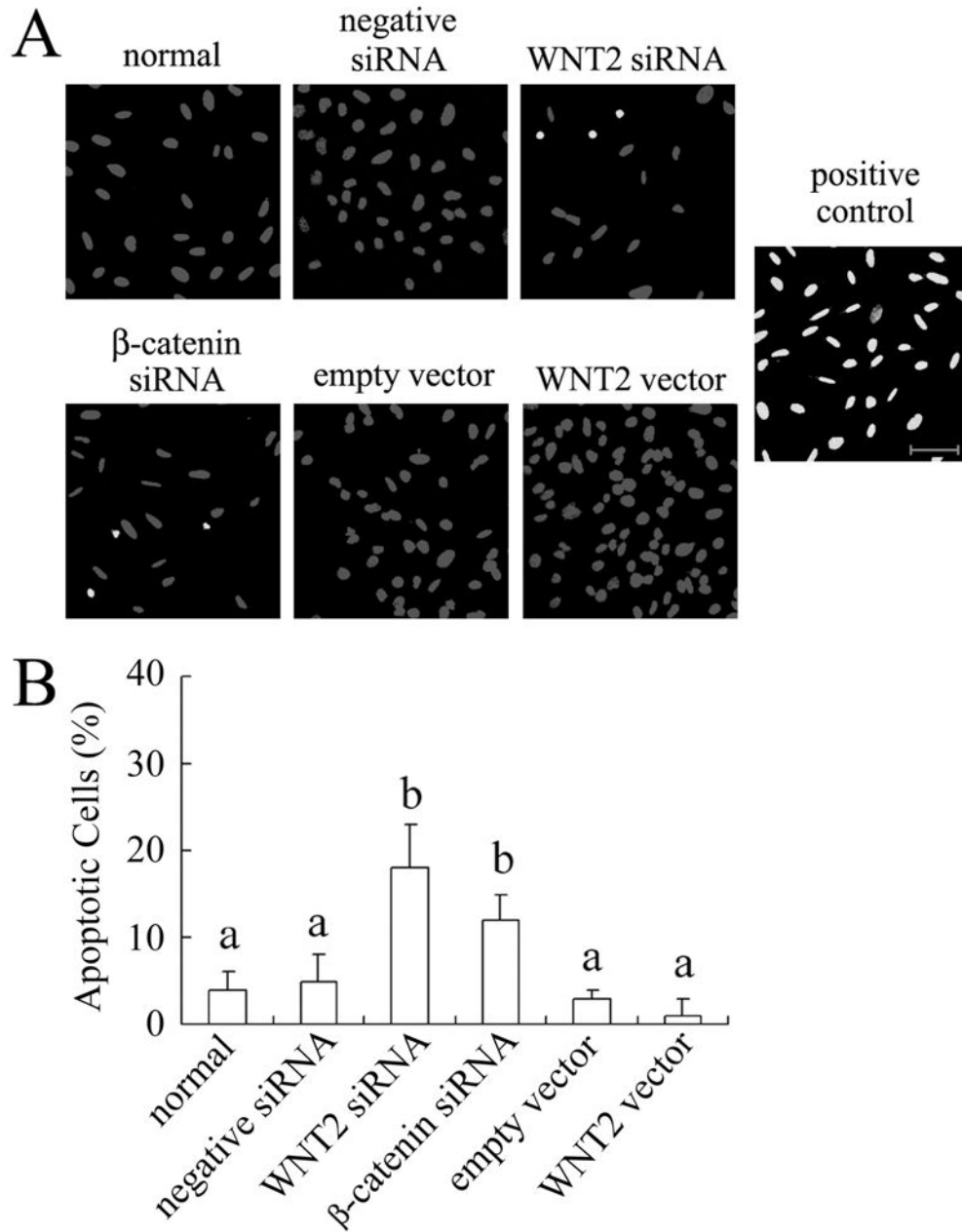


**FIG. 8.** WNT2/ $\beta$ -catenin signaling has a modest effect on apoptosis of granulosa cells. (A) Detection of apoptosis in granulosa cells using the TUNEL assay. Scale bar = 50  $\mu$ m. (B) Graphical summary of TUNEL assay data for the different treatments. For the positive control (DNase treatment), 100% of the cells were TUNEL positive.

Table 1

## Antibodies

Antibody	References	Source	Application <sup>a</sup>		
			IF	IB	IP
Goat anti-WNT2	27	BioVision		1: 200	
Goat anti-WNT2	16, 28	Santa Cruz	1: 75	1: 200	4.0 μ
Rabbit anti-GSK-3β	30, 31	Santa Cruz	1: 100	1: 300	
Rabbit anti-β-catenin	32, 33	Chemicon	1:500	1: 1,000	
Mouse anti-PCNA	34	Sigma		1: 1,500	
Rabbit anti-cyclin D2	29	Santa Cruz		1: 500	
Alexa Fluor® 488 goat anti-rabbit		Molecular Probes	1:500		
Alexa Fluor® 488 goat anti-mouse		Molecular Probes	1:500		
Alexa Fluor® 488 rabbit anti-goat		Molecular Probes	1:500		
Alexa Fluor® 594 goat anti-rabbit		Molecular Probes	1:300		
Alexa Fluor® 594 goat anti-mouse		Molecular Probes	1:300		
Alexa Fluor® 680 goat anti-rabbit		Molecular Probes		1: 10,000	
Alexa Fluor® 680 donkey-anti goat		Molecular Probes		1: 10,000	
Alexa Fluor® 680 goat anti-mouse		Molecular Probes		1: 10,000	

<sup>a</sup>IF, immunofluorescence; IB, immunoblotting; IP, immunoprecipitation